超声诊断或治疗用微/纳泡的研究进展

安青青[1], 李晨曦[1], 杨少坤[1], 何晓明[1], 王岳恒[2], 何朝星[1*], 向 柏[1*]

(1. 河北医科大学药学院, 河北 石家庄 050017; 2. 河北医科大学第二医院, 河北 石家庄 050000)

摘要: 过去几十年中, 微泡作为超声造影剂广泛应用于肿瘤成像领域, 随着研究的逐渐深入, 超声靶向微泡破坏技术结合载药微泡能够实现药物的精准释放, 发挥治疗作用。微泡作为微米级载体难以透过肿瘤内皮细胞间隙, 纳米级递药系统——纳泡应运而生, 两者结构特征相似, 但尺寸上的差异突显出纳泡在药物递送方面独特的优势。本综述以外壳材料为分类原则, 对用作超声诊断或治疗的微/纳泡进行归纳总结, 并探讨其未来可能的发展方向, 为微/纳泡的后续开发提供参考。

关键词: 超声造影剂; 微泡; 纳泡; 超声靶向微泡破坏; 诊断; 治疗

中图分类号: R943 **文献标识码**: A **文章编号**: 0513-4870(2024)03-0581-10

Research progress in micro/nanobubbles for ultrasound diagnosis or treatment

AN Qing-qing[1], LI Chen-xi[1], YANG Shao-kun[1], HE Xiao-ming[1], WANG Yue-heng[2], HE Chao-xing[1*], XIANG Bai[1*]

(*1. School of Pharmacy, Hebei Medical University, Shijiazhuang 050017, China; 2. The Second Hospital of Hebei Medical University, Shijiazhuang 050000, China*)

Abstract: In the past few decades, microbubbles were widely used as ultrasound contrast agents in the field of tumor imaging. With the development of research, ultrasound targeted microbubble destruction technology combined with drug-loaded microbubbles can achieve precise drug release and play a therapeutic role. As a micron-scale carrier, microbubbles are difficult to penetrate the endothelial cell space of tumors, and nano-scale drug delivery system—nanobubbles came into being. The structure of the two is similar, but the difference in size highlights the unique advantages of nanobubbles in drug delivery. Based on the classification principle of shell materials, this review summarized micro/nanobubbles used for ultrasound diagnosis or treatment and discussed the possible development directions, providing references for the subsequent development.

Key words: ultrasound contrast agent; microbubble; nanobubble; ultrasound targeted microbubble destruction; diagnosis; therapy

近年来, 研究者致力于开发无创并能够进行精准治疗的递送系统, 超声波以独特的理化性质增加药物的渗透性并促进其释放[1]。微泡 (microbubbles, MBs) 作为传统的超声造影剂, 直径在1～10 μm[2], 能够随血液循环到达各组织器官, 其内部气体的高压缩性及在声场中独特的非线性振荡, 使MBs与周围的组织及血液具有不同的特征, 因此能在低组织背景下成像[3]。但在肿瘤组织中, 内皮细胞的间隙仅允许小于700 nm的颗粒通过, MBs的尺寸限制了其应用, 因此考虑缩小MBs的尺寸将其制成纳泡 (nanobubbles, NBs), 以实

收稿日期: 2023-07-14; 修回日期: 2024-01-22.

基金项目: 国家自然科学基金资助项目 (81973251); 河北省引进留学人员资助项目(C20230351); 河北省2021年度医学科学研究课题 (20211108).

*通讯作者 Tel: 86-311-86265591,

E-mail: chaoxinghe@hebmu.edu.cn; baixiang@hebmu.edu.cn

DOI: 10.16438/j.0513-4870.2023-0873

现肿瘤部位的超声成像和药物递送[4]。超声靶向微/纳泡破坏 (ultrasound targeted microbubble/nanobubble destruction, UTMD/UTND) 在特定部位对体内微/纳泡进行低频超声照射, 气泡产生空化作用并破裂, 释放药物以发挥治疗作用[5], UTMD/UTND 凭借其非侵入性、靶向递送药物的优势得到广泛应用。

微/纳泡均由外壳材料和内部气芯两部分组成, 常采用薄膜水化法、超声法及微流控技术等进行制备[6], 使用聚乙二醇 (polyethylene glycol, PEG) 连接、碳二亚胺偶联、生物素−链霉亲和素偶联等连接方式在其表面连接配体, 使制得的微/纳泡具有靶向性, 在药物递送过程中能够减轻对其他器官或组织的伤害 (图 1)。目前, 微/纳泡外壳材料的研究以脂质居多, 也有聚合物、仿生材料和蛋白质外壳。脂质具有良好的生物相容性, 磷脂基团自组装成高度有序的单层, 产生极低的表面张力, 可得到较为稳定的微/纳泡[7]; 聚合物外壳具有生物可降解的特点, 在体内发挥作用后可降解为气体, 对人体无害; 仿生细胞膜具有良好的生物相容性、长保留时间和天然靶向能力, 可作为多种疾病的治疗系统。回溯近 10 年文献, 按照外壳材料和负载药物类型的不同, 对用于诊疗的微/纳泡研究现状进行综述, 以期为新的开发策略提供参考。

1 微泡

1.1 脂质外壳

1.1.1 非载药微泡 脂质材料种类繁多, 有研究者通过筛选不同脂材以提高 MBs 的稳定性。van Rooij 等[8]分别使用二硬脂酰基磷脂酰胆碱 (1, 2-distearoyl-*sn*-glycero-3-phosphocholine, DSPC) 和二棕榈酰磷脂酰胆碱 (1, 2-dipalmitoyl-*sn*-glycero-3-phosphocholine, DPPC) 两种脂质制备 MBs, 通过考察声学稳定性、振荡行为及外壳性质, 发现 DSPC 制得的 MBs 更稳定, 壳弹性更好, 非线性响应更高, 有利于超声成像。另外, Maruyama 等[9]评估了脂质微泡 (lipid microbubble, LMB) 中磷脂成分对血流成像的影响, 结果表明在 LMB 外壳中添加 60% 的二硬脂酰磷脂酰甘油 (1, 2-distearoyl-*sn*-glycero-3-phospho-glycerol, DSPG) 可提高 LMB 的稳定性, 并延长血流成像时间。由此可见, 脂材的选择对微泡的稳定性至关重要。

也有学者在脂质材料中加入其他物质以增强 MBs 透过血脑屏障 (blood-brain barrier, BBB) 的能力或提高其靶向性。例如, Vince 等[10]将溶菌酶加入磷脂外壳材料中制备 MBs, 通过钆喷替酸葡甲胺 (gadopentetic acid, Gd-DTPA) 外渗的磁共振成像和脑组织组织学检查来测量 BBB 通透性, 结果表明: 在不增加超声压力幅度的情况下, BBB 打开效率提高两倍; Zhao 等[11]制备了磷脂酰丝氨酸 (phosphatidylserine, PS) 修饰的 MBs, PS 作为外壳成分不仅增强壳的稳定性, 也使 MBs 具有靶向性, 通过与 UTMD 结合可安全打开 BBB, 为进一步在脑缺血区域实施靶向药物递送和炎症成像提供基础; Burns 等[12]将透明质酸 (hyaluronic acid, HA) 聚合物附着到磷脂壳上, HA 与 pH 敏感交联剂交联, 生成水凝胶, 通过亮场和荧光显微镜评估证实该 MBs 可靶向高度表达 CD44 的人类恶性宫颈癌细胞; Liu 等[13]将磁性纳米颗粒与 MBs 结合成功制备磁性 MBs, 在荷瘤小鼠肿瘤周围放置磁铁, 静脉注射 MBs 后, 在接近磁铁的部位观察到很强的荧光信号, 说明 MBs 定向聚集在靶部位。

1.1.2 负载化学药物的微泡 Ren 等[14]使用冷冻干燥技术将多西他赛 (docetaxel, DOC) 包封于脂质 MBs 中制备成冻干粉, 静脉注射后, 通过与 UTMD 结合释放药物。肿瘤细胞生长抑制率实验表明药物局部递送增加, 抗肿瘤效果显著。Lin 等[15]首次合成负载肝素的 MBs, 与 UTMD 结合显著减轻急性胰腺炎大鼠的氧化应激, 从而减少炎症。负载药物的 MBs 虽然可以作为

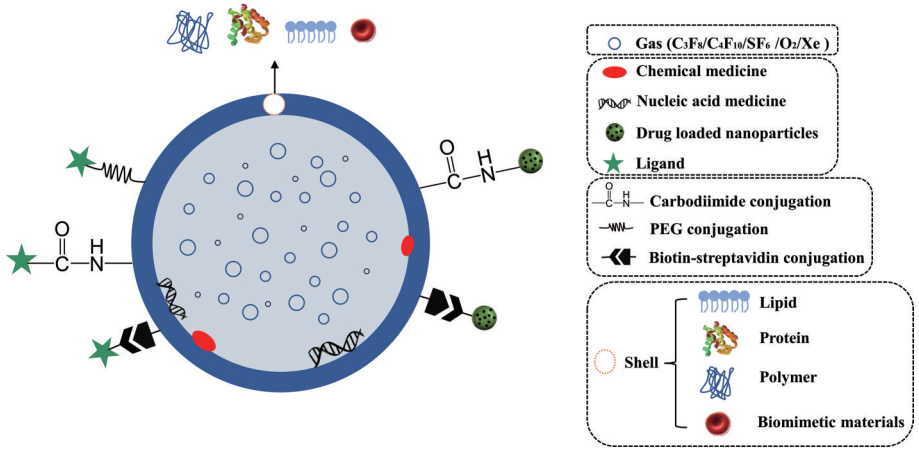

Figure 1 The structure diagram of micro/nanobubble

载体递送药物, 但不具有靶向性, 药物无法在靶部位释放实现精准治疗。Feng等[16]制备的负载雷公藤甲素(triptolide, T_{10}) 并修饰有桥粒连接蛋白 (recombinant desmoyokin, AHNAK) 的靶向MBs用于缓解帕金森病的运动障碍, AHNAK促进MBs在脑血管壁附近积聚, 聚焦超声暴露引起的气泡空化可同时诱导药物释放和BBB打开, 两者结合显著提高T_{10}的脑内浓度。

除连接配体对MBs进行修饰外, 通过将载药纳米粒与MBs偶联, 可提高MBs的载药能力并增强超声信号。Moon等[17]将包封紫杉醇 (paclitaxel, PTX) 的人血清白蛋白纳米颗粒与MBs进行偶联, 静脉注射该微泡并暴露于超声下的小鼠具有更高的存活率。也有学者[18]开发负载多柔比星 (doxorubicin, DOX) 的白蛋白纳米颗粒与MBs的共轭复合物, 保存在碘油乳剂介质中。当MBs到达肿瘤部位时, 通过超声触发产生长期治疗效果, 其释放速度缓慢, 如果药物在循环过程中泄露, 可将不良反应降到最低。

1.1.3 负载核酸药物的微泡 基因药物是具有生物活性的物质, 在体内不经过肝肾代谢, 对人体毒副作用较小。近年来许多学者将基因药物与MBs结合以实现癌症的诊疗一体。Kopechek等[19]将一种寡核苷酸修饰在MBs表面, 该寡核苷酸是信号转导和转录激活因子3 (signal transducer and activator of transcription 3, STAT3) 诱饵, 能够减少核酸酶的降解并以高亲和力结合STAT3蛋白, 阻止其信号传导, 从而抑制肿瘤细胞生长, 同时动物实验证实UTMD与MBs结合能够促进STAT3诱饵在靶部位的聚集和释放。

表1[8-19]对3种不同类型的脂质外壳微泡进行了总结。

1.2 仿生材料外壳

与常规的制备材料相比, 细胞膜等仿生材料具有安全、免疫原性低等优点, 常通过细胞膜与脂材混合作为外壳, 填充气体制备微泡。有学者使用中性粒细胞膜[20]或大脑微血管细胞膜[21]与脂质以一定比例混合, 得到的微泡体内稳定性、生物相容性和靶向能力均较好。Xu等[22]将血小板膜与聚合物材料混合制备微泡, 利用血小板膜天然的归巢作用优化其靶向能力, 用于检测心肌缺血再灌注损伤。

1.3 其他外壳

近年来, 蛋白质与聚合物外壳MBs研究较少。有学者使用白蛋白和5-氟尿嘧啶制备MBs, 通过超声介导的微泡空化增加细胞膜通透性, 释放药物后增加其进入肿瘤细胞的概率[23]。也有研究者通过乙醇–水交换法制备具有超稳定的三层结构蛋白质外壳微泡, 制

Table 1 Lipid microbubbles. DSPC: 1,2-Distearoyl-*sn*-glycero-3-phosphocholine; DPPC: 1,2-Dipalmitoyl-*sn*-glycero-3-phosphocholine; DSPG: 1,2-Distearoyl-*sn*-glycero-3-phospho-glycerol; DSPE: 1,2-Distearoyl-*sn*-glycero-3-phosphoethanolamine; PEG: Polyethylene glycol; DBPC: 1,2-Dibehenoyl-*sn*-glycero-3-phosphocholine; PEG40: Polyethylene glycol 40; DPPS: 1,2-Dipalmitoyl-*sn*-glycero-3-phospho-*L*-serine; DOC: Docetaxel; HSPC: 1,2-Diacyl-*sn*-glycerol-3-phosphocholine; T_{10}: Triptolide; AHNAK: Recombinant desmoyokin; PEG2000: Polyethylene glycol 2000; NHS: N-Hydroxy succinimide; PTX: Paclitaxel; DOX: Doxorubicin; STAT3: Signal transducer and activator of transcription 3

Shell material	Medicine	Ligand	Synthesis method	Connection	Size/μm	Application	Ref.
DSPC/DPPC	-	-	Sonication	-	2−10	Ultrasonic imaging	[8]
DSPC, DSPG, DSPE-PEG-2000	-	-	Thin-film hydration	-	2.5	Ultrasonic imaging	[9]
DBPC, PEG40	-	-	Mechanical shaking	-	-	Enhance ultrasound-mediated BBB breakdown	[10]
DSPC, DSPE-PEG-2000, DPPS	-	-	Sonication	-	4.3 ± 1.1	Enhance ultrasound-mediated BBB breakdown	[11]
Lipids	-	-	Thin-film hydration	-	3.02 ± 0.28	Diagnosis of malignant cervical cancer	[12]
DSPC, DSPE-PEG-2000	-	-	Thin-film hydration	-	2.55 ± 0.14	Ultrasonic imaging	[13]
DPPC-Na, DSPC	DOC	-	Sonication	-	3.39 ± 0.01	Diagnosis and treatment of cancer	[14]
HSPC, DSPC	Heparin sodium	-	Sonication	-	3.46 ± 0.12	Treatment of acute pancreatic cancer	[15]
Dipalmitoyl phosphatidylcholine, DSPE-PEG-2000	T_{10}	AHNAK	Thin-film hydration	Biotin-streptavidin conjugation	1.67 ± 0.24	Alleviating motor deficit of Parkinson's disease	[16]
DSPC, DSPE-PEG2000-NHS	PTX	-	Reversed-phase evaporation	Carbodiimide conjugation	1.1 ± 0.5	Diagnosis and treatment of cancer	[17]
DSPE-PEG2000-NHS, DSPC	DOX	-	Thin-film hydration	Carbodiimide conjugation	1.24 ± 0.17	Diagnosis and treatment of cancer	[18]
DSPC, DSPE-PEG2000	STAT3 decoy	-	Thin-film hydration	-	2.2 ± 1.1	Diagnosis and treatment of cancer	[19]

剂本身及在体内、外超声照射下均较SonoVue稳定[24]。

Delaney等[25]制备聚乙二醇化聚乳酸外壳包封吉西他滨 (gemcitabine, GEM) 的MBs用于治疗胰腺癌。通过评估破坏性脉冲前后的增强差异, 确认肿瘤内MBs的破坏, 表明MBs能够通过超声触发递送GEM。但肿瘤生长没有明显减少, 该团队推测载药MBs递送到肿瘤组织的药量不足, 后续将通过共同包封载药纳米颗粒增加GEM的负载量, 提高肿瘤治疗效果。

2 纳泡

MBs直径较大, 无法进入毛细血管丰富的器官或组织, 而纳泡直径通常在1 000 nm以下, 由于尺寸较小, 能够通过肿瘤血管内皮间隙, 在肿瘤血管内皮部位的高渗透性和滞留效应 (enhanced permeability and retention, EPR) 下被动靶向到肿瘤部位发挥成像及治疗作用[3]。

2.1 脂质外壳

2.1.1 非载药纳泡 PEG及其各种衍生物由于能够降低磷脂壳的表面张力广泛应用在NBs的制备过程中, Khan等[26]通过改变磷脂和PEG的比例研究氧纳泡的大小和分布, 随PEG比例增加, 氧纳泡直径减小, 对肿瘤的EPR随之增强。当磷脂和PEG的比例为85∶15, NBs具有良好的稳定性, 在高频率超声成像中显示出更高的对比度。Perera等[27]将*N*, *N*-二乙基丙烯酰胺和*N*, *N*-双 (丙烯酰基) 胱胺交联形成网状结构, 结合到脂质外壳中。交联剂的加入既能提高NBs稳定性又能保持膜的柔性, 减少气体扩散。体内超声生物分布实验表明NBs能够改善对肿瘤的渗透性, 肿瘤成像效果增强2倍。Liu等[28]通过调节硅杂化脂材的比例来控制NBs尺寸, 所得NBs的大小随硅杂化脂质量的减少而增加。体内外超声成像实验表明, 硅修饰的NBs显著提高了超声造影能力。

乳腺癌多发于女性群体中, 是最常见的恶性肿瘤之一[29], 人表皮生长因子受体2 (human epidermal growth factor receptor 2, HER2) 和CXC趋化因子受体4 (CXC chemokine receptor type 4, CXCR4) 在乳腺癌肿瘤中过度表达, 常作为药物结合的靶点。Jiang等[30]制备Herceptin偶联的磷脂壳NBs用于靶向乳腺癌HER2阳性细胞, 能够有效穿透肿瘤组织, 延长体内保留时间, 大大改善超声质量, 制备过程中DSPE-PEG2000-COOH作为连接脂质, 有效降低细胞毒性, 避免传统链霉亲和素/生物素系统所导致的免疫原性。有学者将生物素化抗ErbB2 Affibody®分子结合到脂质NBs表面用于靶向HER2过度表达的乳腺癌细胞, 离体荧光成像和激光共聚焦显微镜证实了NBs的靶向性[31]。另有学者将生物素化的膜联蛋白V (annexin V, AV) 偶联在纳泡上制备得到AV-NBs, 通过AV对PS强大的亲和力来进行体内细胞凋亡成像[32]。

前列腺癌发病率较高, 是男性群体中的常见癌症, 超声成像技术能够对前列腺癌进行早期诊断提高患者生存率。有学者制备前列腺特异性膜抗原单链可变片段 (prostate specific membrane antigen scFv, PSMA scFv) 负载的NBs, PSMA scFv分子量较小, 确保靶向NBs有较小的直径穿过肿瘤脉管系统并到达肿瘤细胞[33]。PEG的加入有效延长NBs在肿瘤部位的超声成像时间。Fan等[34]通过生物素−链霉亲和素系统构建了特异性抗PSMA纳米体耦合的NBs, 可特异性黏附到前列腺癌细胞上, 峰值强度更高, 持续时间更长。Wang等[35]制备了携带吲哚青绿 (indocyanine green, ICG) 且表面连接PSMA结合肽的纳泡, 靶向PSMA, 增强前列腺癌超声、光声和荧光成像。ICG的加入不仅能够利用光诱导超声成像, 而且还可以利用其自身的红色荧光用于荧光成像, 使NBs具有多功能成像作用, 精确诊断前列腺癌。

除乳腺癌和前列腺癌之外, NBs也用于其他癌症或疾病的超声诊断。有学者制备CA-125抗体靶向NBs用于诊断卵巢癌[36]。该NBs直径小于100 nm, 在卵巢癌肿瘤细胞内快速积聚, 能够有效延长滞留时间及回声。碳酸酐酶IX (carbonic anhydrase IX, CA IX) 在各种恶性实体瘤的细胞膜上高度表达, 可以作为纳泡结合的良好靶点。Zhu等[37]首次构建了CAⅨ多肽修饰的NBs用于靶向多种恶性肿瘤, 其粒径均匀、安全性好且稳定。Zhang等[38]将抗血管内皮细胞生长因子受体-2配体与NBs偶联用于动脉粥样硬化斑块的超声成像, NBs通过被动靶向和主动靶向到达作用部位, 流式细胞术证实其与特异性配体具有高结合效率。Liu等[39]制备携带抗CD3抗体的纳泡靶向T淋巴细胞, 检测心脏移植中的急性排斥反应。

2.1.2 负载小分子化疗药物的纳泡 载药NBs结合UTND技术能同时实现超声诊断和治疗作用。Lan等[40]开发了负载ICG和PTX的多功能纳泡, 通过UTND实现药物的靶向释放, 并在空化作用下增强细胞膜的通透性, 便于药物进入肿瘤细胞发挥治疗作用, 同时ICG的荧光成像有利于癌症的准确诊断。乳腺肿瘤细胞膜上高度表达CXCR4, AMD070作为CXCR4的拮抗剂, 在体内通过主动靶向作用聚集在CXCR4阳性肿瘤部位, 阻断肿瘤的生长和转移。Shen等[41]制备的携带有AMD070和ICG的靶向NBs用于乳腺癌的多功能成像, 通过超声照射增强肿瘤细胞膜的通透性并释放AMD070, 有效抑制并阻断基质细胞衍生因子1 (stromal cell-derived factor-1, SDF-1)/CXCR4通路的

活性, 促进肿瘤细胞凋亡。Peng等[42]制备了负载PTX的NBs, 并在表面连接AMD070, AMD070既具有靶向性, 又能够在超声照射下与PTX发挥双重抗肿瘤作用。Hamarat等[43]将培美曲塞和帕佐帕尼两种药物结合在磁性纳米粒子上, 并将其制备成磁响应性NBs。磁体存在时, 小鼠体内的荧光聚集在肿瘤部位, 经超声破坏后, 释放两种药物, 协同治疗非小细胞型肺癌。自聚集体是将疏水部分连接到亲水聚合物上时, 自发组装形成纳米尺寸的一种结构。Chung等[44]利用乙二醇壳聚糖自聚集体负载疏水性药物DOC, 并将其偶联在NBs面形成NBs复合物, 超声闪光照射显示, NBs破裂的声蒸发效应可显著增强该复合物的内化, 从而增强药物递送。

载药NBs表面连接有靶向作用的叶酸 (folic acid, FA) 配体将大大提高药物疗效。FA是内源性物质, 缺乏免疫原性, 能够与肿瘤细胞表面高表达的FA受体发生强的相互作用, 从而赋予NBs较高的特异性。Gao等[45]制备负载青蒿琥酯的FA偶联脂质NBs, 用于成像引导的肿瘤靶向化疗。小鼠体内成像显示随注射时间延长, 肿瘤超声信号明显增强, 表明该NBs可作为超声探针实时追踪药物在体内的递送情况。另有学者构建了一种负载低分子量透明质酸 (low molecular weight hyaluronic acid, LMW-HA) 的FA结合纳泡[46], FA与肿瘤相关巨噬细胞 (tumor-associated macrophages, TAMs) 表面的叶酸受体结合, 靶向聚集并释放LMW-HA后能够促进TAMs表型从M2转变为M1型, 抑制肿瘤细胞浸润, 保护组织器官免受外来物质的侵袭。Shen等[47]开发FA和IR-780分子修饰的NBs, 通过增强对比超声成像和近红外荧光成像以精确检测肿瘤, 在808 nm照射的病变中诱导靶向光热治疗, 离体实验进一步证实, FA-NBs-IR780有效诱导肿瘤细胞凋亡并抑制肿瘤生长。

除叶酸外, 单克隆抗体、多肽等物质也可作为配体与体内的靶点特异性结合。Chen等[48]制备了由生物素–链霉亲和素桥接的NBs, 以负载程序性死亡配体1单克隆抗体 (programmed death ligand 1 monoclonal antibody, PD-L1mAb) 和化疗剂DOX, DOX还作为一种声敏剂, 在低强度超声刺激下促进线粒体氧化损伤, 诱导细胞凋亡, 协同免疫疗法、化疗与声动力学疗法有效治疗肝癌。Guo等[49]使用新型FH肽修饰负载DOX的纳泡, 用于靶向肿瘤相关成纤维细胞 (cancer-associated fibroblasts, CAFs) 上高度表达的肌腱蛋白C, 通过超声汽化作用实现DOX的靶向释放, 可根除CAFs并重塑肿瘤微环境。还有学者制备了负载替西罗莫司 (temsirolimus, TEM) 的NBs, 由生物素–链霉亲和素桥接抗G250纳米体在NBs表面, 靶向高度表达G250抗原的肾癌细胞, 结合UTND将NBs在特定部位破坏, 释放TEM后抑制癌细胞生长和转移[50]。

2.1.3 负载生物大分子药物的纳泡 基因药物对人体的特定组织或器官具有高度特异性, 负载基因药物的NBs与超声照射结合能够实现药物靶向递送。Su等[51]制备超声敏感的PDLIM5 siRNA NBs用于对抗非小细胞型肺癌的耐药性。超声照射下, NBs显示出siRNA的可控释放能力, 显著提高siRNA转染效率, 阻断癌细胞增殖并促进其凋亡, 在体外显示出极强的抗癌效果。Liufu等[52]采用薄膜水合法制备聚乙二醇-SS-聚乙烯亚胺纳米颗粒负载DNA的NBs用于诊断和治疗乳腺癌, PEG化的二硫键屏蔽聚乙烯亚胺 (polyethylenimines, PEI) 表面正电荷以提高基因转染效率, EPR使NBs在体内被动靶向到肿瘤细胞, 细胞中大量存在的谷胱甘肽迅速切割PEG, 在超声的作用下, PEI/DNA纳米粒子可以通过声穿孔和内体逃逸进入癌细胞释放DNA。

蛋白质类药物也被用于纳泡研究: Tan等[53]制备了含有可溶性程序性细胞死亡蛋白1 (soluble programmed cell death protein 1, sPD-1) 和二氢卟吩e6 (chlorin e6, Ce6) 的多功能纳泡, 纳泡到达靶部位后释放sPD-1与Ce6, sPD-1充当免疫检查点抑制剂, 能够下调肿瘤细胞中PD-L1的表达, 阻断PD-1/PD-L1信号通路, 改善肿瘤抑制作用, 激活Ce6诱导声动力疗法, 协同免疫治疗作用以增强肝癌治疗效果。

表2对3种不同类型的脂质外壳纳泡进行了总结。

2.2 仿生材料外壳

近来, 研究者们多以血小板膜为材料制备纳泡, 其表面天然存在的蛋白配体对动脉粥样硬化斑块[54]及损伤血管[55]有高度亲和力, NBs随时间的推移积累并合并成更大的气泡, 从而在诊断中产生超声增强信号, 有利于疾病的后续治疗。仿生囊泡作为一种新型材料也可以用作NBs的外壳。有学者将喜树碱包封在仿生双层囊泡中, 填充六氟化硫气体制备成NBs, 并在NBs表面修饰黏蛋白1 (mucin1, MUC1) 配体, 靶向高表达MUC1的肿瘤细胞[56]。与非靶向纳泡相比, 该NBs对MUC1阳性的癌细胞具有更高的细胞摄取能力和更强的细胞毒性。

2.3 其他外壳

聚乳酸–乙醇酸 [poly(lactide-co-glycolic acid), PLGA] 是目前FDA批准可用于制备NBs外壳的聚合物[57]。PLGA经三羧酸循环代谢后产物为水和二氧化碳, 对人体无毒。以PLGA为外壳制备纳泡, 在其表面接枝A10-3.2[58]或成纤维细胞生长因子21[59]等配体能

Table 2 Lipid nanobubbles. DPPA: 1,2-Dipalmitoyl-*sn*-glycero-3-phosphate; DPPE: 1,2-Dipalmitoyl-*sn*-glycero-3-phosphoethanolamine; mPEG-DSPE: 1,2-Distearoyl-phosphatidylethanol amine-methyl-poly ethylene glycol conjugate-2000; AV: Annexin V; PSMA scFv: Prostate specific membrane antigen scFv; CAIX: Carbonic anhydrase IX ; DMPC: 1, 2-Dimyristoyl-*sn*-glycero-3-phosphocholine; VEGFR-2: Vascular endothelial growth factor receptor 2; DPPG: 1,2-Dipalmitoyl-*sn*-glycero-3-phosphorylglycerol; DOPC: 1,2-Dioleyl-*sn*-glycero-3-phosphatidyl choline; FA: Folic acid; LMW-HA: Low molecular weight hyaluronic acid; PD-L1 mAb: Programmed death ligand 1 monoclonal antibody; FITC: Fluorescein isothiocyanate; TEM: Temsirolimus; DPTAP: 1, 2-Dipalmitoyl-3-trimethylammonium-propane; Ce6: Chlorin e6; sPD-1: Soluble programmed cell death protein 1

Shell material	Medicine	Ligand	Synthesis method	Connection	Size / μm	Application	Ref.
DSPC, DSPE-PEG-2000	-	-	Thin-film hydration	-	0.173 ± 0.025	Ultrasonic imaging	[26]
DPPC, DPPA, DPPE, mPEG-DSPE	-	-	Thin-film hydration	-	0.095 ± 0.025	Ultrasonic imaging	[27]
DSPC, DSPE-PEG-2000	-	-	Thin-film hydration	-	0.523 ± 0.046	Ultrasonic imaging	[28]
DPPE, DSPE-PEG-2000	-	Herceptin	Thin-film hydration	Carbodiimide conjugation	0.613 ± 0.025	Diagnosis of breast cancer	[30]
DSPE-PEG-2000, DPPC	-	Biotinylated anti-ErbB2 affibody	Thin-film hydration	Biotin-streptavidin conjugation	0.478 ± 0.030	Diagnosis of breast cancer	[31]
DSPC, DSPE-PEG-2000	-	AV	Thin-film hydration	Biotin-streptavidin conjugation	0.636 ± 0.025	Diagnosis of breast cancer	[32]
DPPC, DSPE-PEG-2000	-	PSMA scFv	Thin-film hydration	Biotin-streptavidin conjugation	0.485 ± 0.028	Diagnosis of prostate cancer	[33]
DPPC, DSPE, DPPA	-	Anti-PSMA nanobody	Thin-film hydration	Biotin-streptavidin conjugation	0.488 ± 0.034	Diagnosis of prostate cancer	[34]
DSPE-PEG-2000, DSPC	-	PSMA-binding peptides	Thin-film hydration	Biotin-streptavidin conjugation	0.192 ± 0.005	Diagnosis of prostate cancer	[35]
DPPC, DPPE, DPPA, DSPE-PEG	-	CA-125	Thin-film hydration	Carbodiimide conjugation	0.075 ± 0.017	Diagnosis of ovarian cancer	[36]
DPPC, DPPG, DPPA	-	CAIX polypeptides	Mechanical shaking	Biotin-streptavidin conjugation	0.504 ± 0.785	Ultrasonic imaging	[37]
DPPC, DSPE-PEG-2000, DMPC	-	VEGFR-2	Ultrasonic emulsion	Biotin-streptavidin conjugation	0.320 ± 0.020	Ultrasound imaging of atherosclerotic plaque	[38]
DSPC, DSPE-PEG-2000	-	CD3 antibody	Thin-film hydration	Biotin-streptavidin conjugation	0.457 ± 0.053	Detecting T lymphocyte infiltration in acute rejection	[39]
DPPC, DPPE, DPPG, DPPA, DSPE-PEG-2000	PTX	-	Mechanical shaking	-	0.470 ± 0.033	Diagnosis and treatment of cancer	[40]
DSPE-PEG-2000	AMD070	-	Mechanical shaking	-	0.497 ± 0.029	Diagnosis and treatment of cancer	[41]
DPPA, DPPC, DPPE, DPPG, DSPE-PEG-2000	PTX	AMD070	Mechanical shaking	PEG conjugation	0.494 ± 0.061	Treatment of breast cancer	[42]
DPPC, DOPC, cholesterol	Pemetrexed, pazopanib	-	Thin-film hydration	-	0.491 ± 0.130	Treatment of none-small cell lung cancer	[43]
DSPC, DSPE-PEG-2000-NHS	DOC	-	Sonication	Carbodiimide conjugation	0.323 ± 0.027	Diagnosis and treatment of cancer	[44]
DSPC, DSPE-PEG-2000	Artesunate	FA	Mechanical shaking	PEG conjugation	0.781 ± 0.005	Diagnosis and treatment of cancer	[45]
DSPE-PEG-2000, DPPC	LMW-HA	FA	Mechanical shaking	PEG conjugation	0.342	Inhibiting tumor cell infiltration	[46]
DPPC, DSPE-PEG-2000	IR-780	FA	Thin-film hydration	PEG conjugation	0.591 ± 0.052	Diagnosis and treatment of cancer	[47]
DPPC, DSPE-PEG-2000, cholesterol	DOX	PD-L1mAb	Thin-film hydration	Biotin-streptavidin conjugation	0.457 ± 0.023	Inducing apoptosis	[48]
DPPC, DSPE-PEG-2000, DSPE-PEG-FITC	DOX	FH peptide	Mechanical shaking	PEG conjugation	0.208	Reshaping the tumor microenvironment	[49]
DPPC, DPPE, DPPG, DPPA, DSPE-PEG-2000	TEM	Anti-G250 nanobodies	Thin-film hydration	Biotin-streptavidin conjugation	0.369 ± 0.043	Diagnosis and treatment of cancer	[50]
DSPE-PEG-2000, DSPC	PDLIM5-siRNA	-	Thin-film hydration	-	0.192 ± 0.005	Treatment of non-small cell lung cancer	[51]
DPPC, DPTAP, DSPE-PEG-2000	pDNA	-	Thin-film hydration	Biotin-streptavidin conjugation	0.502 ± 0.075	Treatment of breast cancer	[52]
DPPC, PEG-2000, cholesterol	Ce6	sPD-1	Thin-film hydration	PEG conjugation	0.283 ± 0.022	Immunotherapy of hepatocellular carcinoma	[53]

够使体系精准到达病灶部位, 结合体外UTND技术, 能够大大提高药物疗效并增强超声成像效果。PLGA具有良好的生物可降解性和亲水性, 但PLGA-NBs小于200 nm时无法在小鼠肿瘤中观察到超声图像[60]。壳聚糖 (chitosan, CS) 因其成本低、相容性好、生物可降解等成为理想的聚合物载体, 且CS外壳比脂质外壳更硬, 与聚丙烯酸共同作为外壳制备的纳泡[61]直径小于100 nm, 体内成像持续时间明显长于目前报道的尺寸小于200 nm的聚合物NBs; 有研究用羧甲基壳聚糖与透明质酸以二硫键连接, 填充八氟丙烷并包载药物制得纳泡, 通过内源性的pH响应和氧化还原响应及外源性的超声刺激能够达到药物释放, 产生良好的抗肿瘤效果[62]。聚甲基丙烯酸 [poly (methacrylicacid), PMAA] 较CS有更优越的生物相容性, 质地柔软, 易制得尺寸较小的纳泡。Li等[63]通过回流沉淀聚合法制备的粒径小于100 nm的单分散聚甲基丙烯酸NBs, 通过EPR被动靶向到肿瘤细胞内。甘氨酸、PEG及RGD修饰在NBs表面, 既提高NBs在水溶液中的分散性, 又降低NBs的细胞毒性, 能够在体内维持较长的循环时间。

脂质与聚合物双层外壳可有效改善外壳的坚硬程度, 提高超声造影能力。Yan等[64]使用PLGA和DSPC两种主要外壳材料通过改良后的双乳液蒸发工艺将姜黄素包裹在NBs内, 用于治疗帕金森病。UTND能够介导BBB打开, 有效促进药物释放, NBs与UTND结合组的帕金森病小鼠模型表现出显著的运动能力。

3 结论与展望

本文综述了脂质、仿生材料、聚合物和蛋白质外壳的微/纳泡在疾病诊断及临床治疗方面的研究, 超声介导的微/纳泡造影剂显现出独特的优势。目前MBs在超声诊断方面应用较多, 由于其声学响应及在体内被破坏后的不可逆性使其应用受限, 几款已经上市的MBs制剂仅用作超声造影剂; NBs因尺寸较小能穿过肿瘤血管的优势成为极具潜力的递药系统, 目前已有进入临床试验阶段的产品[65-67], 但无上市制剂。

由于MBs的应用和随之而来的创新在肿瘤学、心血管疾病等多个领域蓬勃发展, 专业知识的融合和某些实践的标准化对于确保快速发展和未来转化为临床至关重要。有研究者根据疾病需求更改气芯为具有治疗作用的药用气体, 通过微/纳泡递送氙气[68,69]或氧气[70-72], 而气泡脂质体的研究, 更是克服了微泡尺寸大、不稳定且难以将药物递送到深部组织的局限性[73,74]。另有研究者聚焦于微泡与纳泡[75]、纳米粒[76]等复合体的制备, 结合超声治疗脑肿瘤方面的研究, 通过有效开放BBB, 促进第二载体负载药物进入脑内, 靶向配体的连接使其精准定位到脑肿瘤的病灶部位, 大大提高药物疗效。另有科研团队设计超声响应型细菌, 通过超声诱导的短暂热疗促进基因表达, 为细菌介导的免疫治疗提供替代策略[77,78]。新型超声造影剂的发展应当更加关注微/纳泡外壳的优化、药物负载技术及靶向递送策略的开发, 且光动力疗法、光声成像及磁性微/纳泡等联合技术的使用推动微泡的行为操控达到一个新的高度, 实现安全、无创的诊疗一体化将指日可待。

作者贡献: 安青青和何朝星负责文献检索、论文撰写及修改; 向柏负责论文选题、写作指导; 李晨曦和何晓明负责论文校对及结构调整和优化; 王岳恒和杨少坤负责论文的专业性和规范性审阅。

利益冲突: 本文所有作者声明不存在利益冲突关系。

References

[1] Lu SR, Zhao PY, Deng YB, et al. Mechanistic insights and therapeutic delivery through micro/nanobubble-assisted ultrasound [J]. Pharmaceutics, 2022, 14: 480.

[2] Kim K, Lee J, Park MH. Microbubble delivery platform for ultrasound-mediated therapy in brain cancers [J]. Pharmaceutics, 2023, 15: 698.

[3] Cooley MB, Abenojar EC, Wegierak D, et al. Characterization of the interaction of nanobubble ultrasound contrast agents with human blood components [J]. Bioact Mater, 2023, 19: 642-652.

[4] Zhang C, Li YH, Ma XY, et al. Functional micro/nanobubbles for ultrasound medicine and visualizable guidance [J]. Sci China Chem, 2021, 64: 899-914.

[5] Liu SB, Zhang Y, Liu Y, et al. Ultrasound-targeted microbubble destruction remodels tumour microenvironment to improve immunotherapeutic effect [J]. Br J Cancer, 2023, 128: 715-725.

[6] Fournier L, de La Taille T, Chauvierre C. Microbubbles for human diagnosis and therapy [J]. Biomaterials, 2023, 294: 122025.

[7] Gharat SK, Godiyal SC, Malusare PP, et al. Microbubbles contrast agents: general overview as diagnostics and therapeutic agent [J]. Curr Drug Targets, 2022, 23: 960-977.

[8] van Rooij T, Luan Y, Renaud G, et al. Non-linear response and viscoelastic properties of lipid-coated microbubbles: DSPC *versus* DPPC [J]. Ultrasound Med Biol, 2015, 41: 1432-1445.

[9] Maruyama T, Sugii M, Omata D, et al. Effect of lipid shell composition in DSPG-based microbubbles on blood flow imaging with ultrasonography [J]. Int J Pharm, 2020, 590: 119886.

[10] Vince O, Peeters S, Johanssen VA, et al. Microbubbles containing lysolipid enhance ultrasound-mediated blood-brain barrier breakdown *in vivo* [J]. Adv Healthc Mater, 2021, 10: e2001343.

[11] Zhao RR, Jiang J, Li HW, et al. Phosphatidylserine-microbubble targeting-activated microglia/macrophage in inflammation combined with ultrasound for breaking through the blood-brain

barrier [J]. J Neuroinflammation, 2018, 15: 334.

[12] Burns MWN, Mattrey RF, Lux J. Microbubbles cloaked with hydrogels as activatable ultrasound contrast agents [J]. ACS Appl Mater Interfaces, 2020, 12: 52298-52306.

[13] Liu Y, Lai X, Zhu Y, et al. Contrast-enhanced ultrasound imaging using long-circulating cationic magnetic microbubbles *in vitro* and *in vivo* validations [J]. Int J Pharm, 2022, 616: 121299.

[14] Ren ST, Liao YR, Kang XN, et al. The antitumor effect of a new docetaxel-loaded microbubble combined with low-frequency ultrasound *in vitro*: preparation and parameter analysis [J]. Pharm Res, 2013, 30: 1574-1585.

[15] Lin LL, Xie SL, Zhao YZ, et al. Ultrasound-induced destruction of heparin-loaded microbubbles attenuates *L*-arginine-induced acute pancreatitis [J]. Eur J Pharm Sci, 2023, 180: 106318.

[16] Feng Y, An R, Zhang YJ, et al. AHNAK-modified microbubbles for the intracranial delivery of triptolide: *in-vitro* and *in-vivo* investigations [J]. Int J Pharm, 2022, 629: 122351.

[17] Moon H, Yoon C, Lee TW, et al. Therapeutic ultrasound contrast agents for the enhancement of tumor diagnosis and tumor therapy [J]. J Biomed Nanotechnol, 2015, 11: 1183-1192.

[18] Kim D, Lee JH, Moon H, et al. Development and evaluation of an ultrasound-triggered microbubble combined transarterial chemoembolization (TACE) formulation on rabbit VX2 liver cancer model [J]. Theranostics, 2021, 11: 79-92.

[19] Kopechek JA, Carson AR, Mctiernan CF, et al. Ultrasound targeted microbubble destruction-mediated delivery of a transcription factor decoy inhibits STAT3 signaling and tumor growth [J]. Theranostics, 2015, 5: 1378-1387.

[20] Zhang Z, Miao XY, Yao WF, et al. Molecular ultrasound imaging of neutrophil membrane-derived biomimetic microbubbles for quantitative evaluation of hepatic ischemia-reperfusion injury [J]. Theranostics, 2021, 11: 6922-6935.

[21] He CS, Wu ZS, Zhuang M, et al. Focused ultrasound-mediated blood-brain barrier opening combined with magnetic targeting cytomembrane based biomimetic microbubbles for glioblastoma therapy [J]. J Nanobiotechnology, 2023, 21: 297.

[22] Xu LL, Chen YH, Jin QF, et al. Biomimetic PLGA microbubbles coated with platelet membranes for early detection of myocardial ischaemia-reperfusion injury [J]. Mol Pharm, 2021, 18: 2974-2985.

[23] Liao AH, Lee YA, Lin DL, et al. Treatment efficacy of low-dose 5-fluorouracil with ultrasound in mediating 5-fluorouracil-loaded microbubble cavitation in head and neck cancer [J]. Drug Deliv, 2023, 30: 1-13.

[24] Deng QR, Mi JM, Dong JP, et al. Superiorly stable three-layer air microbubbles generated by versatile ethanol-water exchange for contrast-enhanced ultrasound theranostics [J]. ACS Nano, 2022, 17: 263-274.

[25] Delaney LJ, Eisenbrey JR, Brown D, et al. Gemcitabine-loaded microbubble system for ultrasound imaging and therapy [J]. Acta Biomater, 2021, 130: 385-394.

[26] Khan MS, Hwang J, Lee K, et al. Surface composition and preparation method for oxygen nanobubbles for drug delivery and ultrasound imaging applications [J]. Nanomaterials (Basel), 2019, 9: 48.

[27] Perera RH, Wu H, Peiris P, et al. Improving performance of nanoscale ultrasound contrast agents using N, N-diethylacrylamide stabilization [J]. Nanomedicine, 2017, 13: 59-67.

[28] Liu J, Zhang B, Li MT, et al. Preparation and characterization of a novel silicon-modified nanobubble [J]. PLoS One, 2017, 12: e0178031.

[29] Bray F, Ferlay J, Soerjomataram I, et al. Global cancer statistics 2018: GLOBOCAN estimates of incidence and mortality worldwide for 36 cancers in 185 countries [J]. CA Cancer J Clin, 2018, 68: 394-424.

[30] Jiang QC, Hao SY, Xiao XY, et al. Production and characterization of a novel long-acting herceptin-targeted nanobubble contrast agent specific for HER-2-positive breast cancers [J]. Breast Cancer, 2016, 23: 445-455.

[31] Yang HL, Cai WB, Xu L, et al. Nanobubble-affibody: novel ultrasound contrast agents for targeted molecular ultrasound imaging of tumor [J]. Biomaterials, 2015, 37: 279-288.

[32] Zhou T, Cai W, Yang H, et al. Annexin V conjugated nanobubbles: a novel ultrasound contrast agent for *in vivo* assessment of the apoptotic response in cancer therapy [J]. J Control Release, 2018, 276: 113-124.

[33] Ding Y, Cao QF, Qian SB, et al. Optimized anti-prostate-specific membrane antigen single-chain variable fragment-loaded nanobubbles as a novel targeted ultrasound contrast agent for the diagnosis of prostate cancer [J]. J Ultrasound Med, 2019, 39: 761-773.

[34] Fan XZ, Wang LF, Guo YL, et al. Ultrasonic nanobubbles carrying anti-PSMA nanobody: construction and application in prostate cancer-targeted imaging [J]. PLoS One, 2015, 10: e0127419.

[35] Wang YX, Lan MM, Shen DJ, et al. Targeted nanobubbles carrying indocyanine green for ultrasound, photoacoustic and fluorescence imaging of prostate cancer [J]. Int J Nanomedicine, 2020, 15: 4289-4309.

[36] Gao Y, Hernandez C, Yuan HX, et al. Ultrasound molecular imaging of ovarian cancer with CA-125 targeted nanobubble contrast agents [J]. Nanomedicine, 2017, 13: 2159-2168.

[37] Zhu LH, Guo YL, Wang LF, et al. Construction of ultrasonic nanobubbles carrying CAIX polypeptides to target carcinoma cells derived from various organs [J]. J Nanobiotechnology, 2017, 15: 63.

[38] Zhang XY, Wu MC, Zhang Y, et al. Molecular imaging of atherosclerotic plaque with lipid nanobubbles as targeted ultrasound contrast agents [J]. Colloids Surf B Biointerfaces, 2020, 189: 110861.

[39] Liu JF, Chen YH, Wang GH, et al. Ultrasound molecular imaging of acute cardiac transplantation rejection using nanobubbles targeted to T lymphocytes [J]. Biomaterials, 2018, 162: 200-207.

[40] Lan MM, Zhu LH, Wang YX, et al. Multifunctional nanobubbles carrying indocyanine green and paclitaxel for molecular imaging and the treatment of prostate cancer [J]. J Nanobiotechnology, 2020, 18: 121.

[41] Shen DJ, Zhu LH, Liu Y, et al. Efficacy evaluation and mechanism study on inhibition of breast cancer cell growth by multimodal targeted nanobubbles carrying AMD070 and ICG [J]. Nanotechnology, 2020, 31: 245102.

[42] Peng YL, Zhu LH, Wang LF, et al. Preparation of nanobubbles modified with a small-molecule CXCR4 antagonist for targeted drug delivery to tumors and enhanced ultrasound molecular imaging [J]. Int J Nanomedicine, 2019, 14: 9139-9157.

[43] Hamarat Şanlıer Ş, Ak G, Yılmaz H, et al. Development of ultrasound-triggered and magnetic-targeted nanobubble system for dual-drug delivery [J]. J Pharm Sci, 2019, 108: 1272-1283.

[44] Chung IJ, Moon H, Jeon SI, et al. Ultrasound-triggered imaging and drug delivery using microbubble-self-aggregate complexes [J]. J Biomater Sci Polym Ed, 2022, 33: 57-76.

[45] Gao S, Cheng XH, Li JH. Lipid nanobubbles as an ultrasound-triggered artesunate delivery system for imaging-guided, tumor-targeted chemotherapy [J]. Onco Targets Ther, 2019, 12: 1841-1850.

[46] Sun X, Guo L, Shang MM, et al. Ultrasound mediated destruction of LMW-HA-loaded and folate-conjugated nanobubble for TAM targeting and reeducation [J]. Int J Nanomedicine, 2020, 15: 1967-1981.

[47] Shen YM, Lv W, Yang HL, et al. FA-NBs-IR780: novel multifunctional nanobubbles as molecule-targeted ultrasound contrast agents for accurate diagnosis and photothermal therapy of cancer [J]. Cancer Lett, 2019, 455: 14-25.

[48] Chen YZ, Luo XQ, Liu Y, et al. Targeted nanobubbles of PD-L1 mAb combined with doxorubicin as a synergistic tumor repressor in hepatocarcinoma [J]. Int J Nanomedicine, 2022, 17: 3989-4008.

[49] Guo L, Shi DD, Meng D, et al. New FH peptide-modified ultrasonic nanobubbles for delivery of doxorubicin to cancer-associated fibroblasts [J]. Nanomedicine, 2019, 14: 2957-2971.

[50] Yu ZP, Wang YX, Xu D, et al. G250 antigen-targeting drug-loaded nanobubbles combined with ultrasound targeted nanobubble destruction: a potential novel treatment for renal cell carcinoma [J]. Int J Nanomedicine, 2020, 15: 81-95.

[51] Su CH, Ren XJ, Yang F, et al. Ultrasound-sensitive siRNA-loaded nanobubbles fabrication and antagonism in drug resistance for NSCLC [J]. Drug Deliv, 2022, 2: 99-110.

[52] Liufu C, Li Y, Tu J, et al. Echogenic pegylated PEI-loaded microbubble as efficient gene delivery system [J]. Int J Nanomedicine, 2019, 14: 8923-8941.

[53] Tan YD, Yang SQ, Ma Y, et al. Nanobubbles containing sPD-1 and Ce6 mediate combination immunotherapy and suppress hepatocellular carcinoma in mice [J]. Int J Nanomedicine, 2021, 16: 3241-3254.

[54] Zhou J, Niu CC, Huang BY, et al. Platelet membrane biomimetic nanoparticles combined with UTMD to improve the stability of atherosclerotic plaques [J]. Front Chem, 2022, 10: 868063.

[55] Li MX, Liu Y, Chen JP, et al. Platelet bio-nanobubbles as microvascular recanalization nanoformulation for acute ischemic stroke lesion theranostics [J]. Theranostics, 2018, 8: 4870-4883.

[56] Ghasemzadeh T, Hasannia M, Abnous K, et al. Preparation of targeted theranostic red blood cell membranes-based nanobubbles for treatment of colon adenocarcinoma [J]. Expert Opin Drug Deliv, 2022, 20: 131-143.

[57] Deng LW, Li L, Yang H, et al. Development and optimization of doxorubicin loaded poly (lactic-co-glycolic acid) nanobubbles for drug delivery into HeLa cells [J]. J Nanosci Nanotechnol, 2014, 14: 2947-2954.

[58] Wu M, Wang Y, Wang YR, et al. Paclitaxel-loaded and A10-3.2 aptamer-targeted poly (lactide-co-glycolic acid) nanobubbles for ultrasound imaging and therapy of prostate cancer [J]. Int J Nanomedicine, 2017, 12: 5313-5330.

[59] Gao JM, Liu JJ, Meng ZY, et al. Ultrasound-assisted C_3F_8-filled PLGA nanobubbles for enhanced FGF21 delivery and improved prophylactic treatment of diabetic cardiomyopathy [J]. Acta Biomater, 2021, 130: 395-408.

[60] Díaz-López R, Tsapis N, Santin M, et al. The performance of pegylated nanocapsules of perfluorooctyl bromide as an ultrasound contrast agent [J]. Biomaterials, 2010, 31: 1723-1731.

[61] Gao X, Guo D, Mao X, et al. Perfluoropentane-filled chitosan poly-acrylic acid nanobubbles with high stability for long-term ultrasound imaging *in vivo* [J]. Nanoscale, 2021, 13: 5333-5343.

[62] Xiao S, Guo L, Ai C, et al. pH-/Redox-responsive nanodroplet combined with ultrasound-targeted microbubble destruction for the targeted treatment of drug-resistant triple negative breast cancer [J]. ACS Appl Mater Interfaces, 2023, 15: 8958-8973.

[63] Li YJ, Wan JX, Zhang ZH, et al. Targeted soft biodegradable glycine/PEG/RGD-modified poly (methacrylic acid) nanobubbles as intelligent theranostic vehicles for drug delivery [J]. ACS Appl Mater Interfaces, 2017, 9: 35604-35612.

[64] Yan YR, Chen Y, Liu ZX, et al. Brain delivery of curcumin through low-intensity ultrasound-induced blood-brain barrier opening *via* lipid-PLGA nanobubbles [J]. Int J Nanomedicine, 2021, 16: 7433-7447.

[65] Oxford University Hospitals NHS Trust. Do nanobubbles improve joint hypoxia? [DB/OL]. Oxford: University of Oxford, 2021[2023-07-14]. https://classic.clinicaltrials.gov/ct2/show/NCT04844008.

[66] Handa A. Oxygen nanobubble drink impact on exercise in elite athletes [DB/OL]. Oxford: University of Oxford, 2023[2023-07-

14]. https://classic.clinicaltrials.gov/ct2/show/NCT05777642.

[67] Vyas R. Micro/nanobubbles (MNBs) for treatment of acute and chronic wounds [DB/OL]. Irvine: University of California, Irvine, 2021 [2023-07-14]. https://classic.clinicaltrials.gov/show/NCT05169814.

[68] Shekhar H, Palaniappan A, Peng T, et al. Characterization and imaging of lipid-shelled microbubbles for ultrasound-triggered release of xenon [J]. Neurotherapeutics, 2019, 16: 878-890.

[69] Jin J, Li M, Li J, et al. Xenon nanobubbles for the image-guided preemptive treatment of acute ischemic stroke *via* neuroprotection and microcirculatory restoration [J]. ACS Appl Mater Interfaces, 2021, 13: 43880-43891.

[70] Drzal A, Delalande A, Dziurman G, et al. Increasing oxygen tension in tumor tissue using ultrasound sensitive O_2 microbubbles [J]. Free Radic Biol Med, 2022, 193: 567-578.

[71] Reusser TD, Song KH, Ramirez D, et al. Phospholipid oxygen microbubbles for image-guided therapy [J]. Nanotheranostics, 2020, 4: 83-90.

[72] Song RY, Peng S, Lin QG, et al. pH-responsive oxygen nanobubbles for spontaneous oxygen delivery in hypoxic tumors [J]. Langmuir, 2019, 35: 10166-10172.

[73] Koebis M, Kiyatake T, Yamaura H, et al. Ultrasound-enhanced delivery of morpholino with bubble liposomes ameliorates the myotonia of myotonic dystrophy model mice [J]. Sci Rep, 2013, 3: 2242.

[74] Negishi Y, Ishii Y, Nirasawa K, et al. PMO delivery system using bubble liposomes and ultrasound exposure for Duchenne muscular dystrophy treatment [J]. Methods Mol Biol, 2018, 1687: 185-192.

[75] Wang F, Dong L, Liang SM, et al. Ultrasound-triggered drug delivery for glioma therapy through gambogic acid-loaded nanobubble-microbubble complexes [J]. Biomed Pharmacother, 2022, 150: 113042.

[76] Wu H, Gao X, Luo Y, et al. Targeted delivery of chemo-sonodynamic therapy *via* brain targeting, glutathione-consumable polymeric nanoparticles for effective brain cancer treatment [J]. Adv Sci, 2022, 9: e2203894.

[77] Abedi MH, Yao MS, Mittelstein DR, et al. Ultrasound-controllable engineered bacteria for cancer immunotherapy [J]. Nat Commun, 2022, 13: 1585.

[78] Chen YH, Du M, Yuan Z, et al. Spatiotemporal control of engineered bacteria to express interferon-γ by focused ultrasound for tumor immunotherapy [J]. Nat Commun, 2022, 13: 4468.